Dynamical Characteristics of Surface EMG Signals of Hand Grasps via Recurrence Plot

Gaoxiang Ouyang, Xiangyang Zhu, Zhaojie Ju, *Member, IEEE*, and Honghai Liu, *Senior Member, IEEE*

***Abstract*—Recognizing human hand grasp movements through surface electromyogram (sEMG) is a challenging task. In this paper, we investigated nonlinear measures based on recurrence plot, as a tool to evaluate the hidden dynamical characteristics of sEMG during four different hand movements. A series of experimental tests in this study show that the dynamical characteristics of sEMG data with recurrence quantification analysis (RQA) can distinguish different hand grasp movements. Meanwhile, adaptive neuro-fuzzy inference system (ANFIS) is applied to evaluate the performance of the aforementioned measures to identify the grasp movements. The experimental results show that the recognition rate (99.1%) based on the combination of linear and nonlinear measures is much higher than those with only linear measures (93.4%) or nonlinear measures (88.1%). These results suggest that the RQA measures might be a potential tool to reveal the sEMG hidden characteristics of hand grasp movements and an effective supplement for the traditional linear grasp recognition methods.**

***Index Terms*—Hand grasp, nonlinear measures, recurrence plot (RP), surface electromyogram (sEMG).**

I. Introduction

THE surface electromyogram (sEMG) reflects both peripheral and central properties of the neuromuscular system and presents information of the neural activation of muscles [1]. Thus, the analysis of the sEMG signals is particularly attractive in that it provides relatively easy access to the physiological processes that allow the muscles to generate force and movement [2], [3]. One important potential application using sEMG signals lies in controlling prosthetic devices [4]–[7], for instance hand prostheses [8], [9], due to the fact that sEMG signals contain the electrical activities of arm muscle contraction that undergo many complex transitions in different hand movements [10]. However, there are inherent difficulties in deriving a general model on the relationship between the recorded sEMG and hand gestures when humans perform contractions [11]. In order to control a prosthetic device, the fundamental challenge is to efficiently handle sEMG signals and identify the intention of the users [12]. Meanwhile, the exploration of inherent features of sEMG signals could be of benefit in understanding the mechanisms of neuromuscular systems. Therefore, there is a growing interest in tackling this challenge [13].

Various methods have been proposed to extract valuable information from sEMG signals ranging from traditional linear methods such as time and frequency analysis to nonlinear methods. In the time domain, traditional methods of EMG amplitude analysis mainly consist of the mean absolute value (MAV), number of zero crossings (ZC), waveform length (WL), and number of slope sign (SS) changes [14], [15]. It should be noted that, during a sustained isometric contraction, there is a phenomenon called EMG spectrum compression. That is to say that there is an increase in the amplitude of the low frequency band and a relative decrease in the higher frequency band [16]. To some extent, these traditional methods of EMG amplitude have the capability of tracking muscular changes [15]. However, traditional methods of sEMG amplitude and spectral analysis are not effective in analyzing complex transient signals [17]. In particular, the spectral analysis is based on an assumption that the observed variations of electrical field of muscle activity are time-invariant (stationary) processes [16]. Therefore, these traditional methods fail to detect the critical feature of sEMG data during transient human movement since this assumption is inconsistent with sEMG dynamics.

Nonlinear methods derived from the theory of nonlinear dynamical systems (also called chaos theory) recently have been proposed to analyze the sEMG signals [16]. These methods such as the Lyapunov exponents and fractal dimension extract the informative features from sEMG data to detect the muscle status changes [18]. However, chaos-based approaches assume that the signal is stationary and originates from a low dimensional nonlinear system [19]. In practice, the sEMG signal is a nonstationary signal and stems from a highly nonlinear system, which is a complex signal embedded in noise [20]. It is thus promising to develop new methods to characterize sEMG changes in different neural activation of muscles based on nonlinear methods. Moreover, recently reported sEMG analysis techniques and tools have made it possible to extract the substantial meaningful information from recordings of the neuromuscular system [16], [21]. Note that chaos-based approaches should be employed to analyze sEMG data in constrained conditions [13].

Manuscript received November 6, 2012; revised February 24, 2013; accepted April 27, 2013. Date of publication May 15, 2013; date of current version December 31, 2013. This work was supported in part by the National Basic Research Program (973 Program) of China under Grant 2011CB013305, in part by Leverhulme Trust under Grant 13754, and in part by U.K. National Engineering and Physical Scientific Research Council under Grant EP/G041377/1.

G. Ouyang and Z. Ju are with the Intelligent Systems and Biomedical Robotics Group, School of Creative Technologies, University of Portsmouth, England, PO1 2DJ, U.K. (e-mail: gx.ouyang@gmail.com; zhaojie.ju@port.ac.uk).

H. Liu is with the Intelligent Systems and Biomedical Robotics Group, School of Creative Technologies, University of Portsmouth, England, PO1 2DJ, U.K. and also with the State Key Laboratory of Mechanical System and Vibration, School of Mechanical Engineering, Shanghai Jiao Tong University, Shanghai 200240, China (e-mail: honghai.liu@port.ac.uk).

X. Zhu is with the State Key Laboratory of Mechanical System and Vibration, School of Mechanical Engineering, Shanghai Jiao Tong University, Shanghai 200240, China (e-mail: mexyzhu@sjtu.edu.cn).

Color versions of one or more of the figures in this paper are available online at http://ieeexplore.ieee.org.

Digital Object Identifier 10.1109/JBHI.2013.2261311

It is evident that nonlinear methods have significantly inspired research in sEMG signal analysis. For instance, a recurrence quantification analysis (RQA) was employed to analyze the nonlinear dynamical characteristics of sEMG data [3]. One of its key features is the ability of describing nonlinear nature of short and nonstationary signal corrupted with noise [22]. RQA methods had been broadly applied to the analysis of physiological data, such as electroencephalogram data [23], fMRI data [24], heart signals [25], and EMG data [26], [27]. A number of experimental studies had showed that RQA methods have high potential of detecting changes in sEMG due to muscle contractions [28] or fatigue [29]. For example, Yuan *et al.* employed RQA measures and BP neural network to classify eight forearm motions, which has been proved to achieve a desirable motion classification accuracy [30]. This study aims to investigate whether or not the RQA measures can extract the sEMG hidden characteristics of hand grasp movements so that it can be employed as an effective supplement for the traditional linear grasp recognition methods.

II. Materials and Methods

Eight (two female, six male) healthy right-handed subjects were volunteered for this study. Their ages range from 23 years old to 40 years old, and on average it is 32.5 years old; the body height on average is 175.5 cm; the body mass on average is 70 kg. All participants were given informed consent prior to the experiments according to the University of Portsmouth CCI Faculty Ethics Committee.

A. Experimental Procedure

The experiment consists of both freely grasps and different grasping gestures. Each type of the grasps was repeated ten times. Every motion lasted about 2 s. Between every two repetitions, participants were instructed to relax their hands for 2 s in the intermediate state, which is the status of opening hand naturally without any muscle contraction. Once one motion with ten repetitions was completed, participants were instructed to relax their hand for 2 min before the next motion started. This was designed to overcome the effects of occurred muscle fatigue.

B. Data Collection

The four EMG electrodes were applied to the subject's right forearm muscles, i.e., flexor carpi radialis (channel 1), flexor carpi ulnaris (channel 2), flex or pollicis longus (channel 3), and flexor digitorum profundus (channel 4). The sEMG data were recorded using DataLINK system from Biometrics LTD with a gel-skin contact area of about 4 cm^2 for each bipolar electrode and a center-to-center recording distance of 20 mm. The sampling frequency of DataLINK system in our experiment was set to be 1000 Hz and sEMG signals were amplified 1000 times and bandwidth is 20 to 460 Hz using a sEMG amplifier (SX230FW sEMG Amplifier, Biometrics, Ltd.). To obtain good-quality signals, subjects were scrubbed with alcohol and shaved if necessary and then electrodes were applied over the body using the die cut medical grade double-sided adhesive tape. Electrodes locations were selected according to the musculoskeletal system

Fig. 1. Three hand grasping tasks.

of these four muscles and confirmed by specific muscle contractions, which include manually resisted finger flexion, extension, and abduction. The captured sEMG signals were visualized on a computer screen in order to provide the participants feedback for their choosing the positions of the electrodes with stronger sEMG signals.

To investigate the dynamical characteristics of sEMG data during different grasp gestures, EMG signals were selected from grasp states of no action (dataset I), grasp, and lift an orange using five fingers (dataset II), grasp, and lift a can full of rice using five fingers with the thumb abduction (dataset III) and hold and lift a dumbbell (dataset IV) intervals as shown in Fig. 1. In this study, 80 4-channel 1 s EMG epochs were selected for each dataset. Short (1 s) EMG signals were used since the duration of the grasp gesture is only about a few seconds. The criterion for the selection of the EMG signals from hand grasps is that the interval is the first 1 s of hand starting to hold and lift the objects.

C. Phase Space Reconstruction

EMG data are nonstationary time series. The first step in the analysis of a signal using nonlinear dynamics theory is the reconstruction of the phase space trajectory of the signal [31]. The methods involving time delay are usually used to embed a scalar time series into a m-dimensional space, it is

$$x_k = (u_k, u_{k+\tau}, \ldots, u_{k+(m-1)\tau}) \tag{1}$$

where $k = 1, 2, \ldots, L-(m-1)\tau$, τ is the delay time, and m is the embedding dimension, $m \geq 2$. The difficulty of this method is the choice of the delay time τ and the minimum embedding dimension, m.

Takens' theorem assumes that the data are infinite and noise free, where the delay time τ can be chosen almost arbitrarily. However, real EMG datasets are always finite and noisy; the choice of the delay time must therefore be carefully considered. If τ is too small, the reconstructed vector is too close to serve as independent coordinates; if τ is too large, the reconstructed vector is independent and loses the connection with each other [32]. The most common method for choosing a proper time delay is based on the detection of the first local minimum of the mutual information (MI) function [33], since the first minimum of the $\mathrm{MI}(\tau)$ portrays the time delay where the signal $u_{t+\tau}$ adds maximal information to the knowledge obtained from u_t [33]. The MI method produces nonlinear characteristics of time series, so it is better to estimate time delay than linear autocorrelation functions.

As for the choice of the embedding dimension, if the m is too small, the geometry is not entirely unfolded. As shown in Takens' embedding theorem, it certainly unfolds the attractor in m-dimensional space when $m < 2d + 1$, where d is the dimension of the attractor defined by the orbits. On the other hand, if m is too large, it leads to excessive computations and enhances the problem of contamination by round off or instrumental error. Hence, it is crucial to choose a sufficiently large embedding dimension that contains the relevant dynamics in the presence of noise. There are a number of different criteria for choosing m presented in the literature. Cao proposed a robust and efficient method that determines the minimum embedding dimension; it can overcome some shortcomings of false nearest neighbors [34]. In this study, the MI method [33] and Cao's method [34] are employed to estimate the delay time and the embedding dimension, respectively.

D. Recurrence Plot and RQA Measures

Recurrence plots (RP), proposed by Eckmann *et al.* [35], describes the recurrence property of a deterministic dynamical system, i.e., visualizing the time-dependent behavior of orbits x_i in a phase space. The key step of RP is to calculate the following $N \times N$ matrix:

$$R_{i,j}(\varepsilon) = \Theta(\varepsilon - \|x_i - x_j\|), i, j = 1, \ldots, N \tag{2}$$

where $N = L - (m-1)\tau$, ε is a predefined cutoff distance, $\|\cdot\|$ is the norm (e.g., the Euclidean norm), and $\Theta(x)$ is a Heaviside function. The phase space vector x_i can be reconstructed using Takens' time delay method, $x_i = (u_i, u_{i+\tau}, \ldots, u_{i+(m-1)\tau})$ [31], based on the observations u_i. The cutoff distance ε defines a sphere centered at x_j, if x_i falls within this sphere, i.e., the state is close to x_j, then $R_{i,j} = 1$; otherwise $R_{i,j} = 0$. The binary values of $R_{i,j}$ can be simply visualized with the colors black (1) and white (0). Thereby, the RP can be considered as a visual inspection of a high-dimensional phase space trajectory: in other words, the RP indicates the time evolution of a trajectory. In short, the RP can describe the characteristics of large-scale and small-scale patterns of a dynamical system [35].

In order to further investigate the properties of the RP, several measures of complexity that quantify the small-scale structures in the RP called RQA have been proposed. We only introduced two measure variables: determinism (DET) and entropy (ENTR) in this paper. These measures are based on the recurrence point density and the diagonal line structures of the RP. For more details please refer to [22].

The classical measure of the RQA is the recurrence rate (RR)

$$\mathrm{RR}(\varepsilon) = \frac{1}{N^2} \sum_{i,j=1}^{N} R_{i,j}(\varepsilon) \tag{3}$$

which simply counts the black dots in the RP. The RR is a measure of the density of recurrence points, and the value

$$N_n(\varepsilon) = \frac{1}{N} \sum_{i,j=1}^{N} R_{i,j}(\varepsilon) \tag{4}$$

is the simple average number of neighbors that each point on the trajectory has in its $\varepsilon-$neighborhood.

The frequency distribution of the lengths l of the diagonal structures in the RP is $P^{\varepsilon}(l) = \{l_i; i = 1, 2, \ldots, N\}$. The ratio of recurrence points on the diagonal structures (of at least length $l_{\min}$) to all recurrence points is called the DET, and is introduced as a determinism (or predictability) measure of the system. Its formulation is given as follows:

$$\mathrm{DET} = \sum_{l=l_{\min}}^{N} lP^{\varepsilon}(l) \Big/ \sum_{l=1}^{N} lP^{\varepsilon}(l) \tag{5}$$

where $l_{\min}$ is the threshold, which excludes the diagonal lines formed by the tangential motion of a phase space trajectory, which in this study we fixed at $l_{\min} = 2$.

The ENTR refers to the Shannon entropy of the frequency distribution of the diagonal line lengths

$$\begin{aligned} \mathrm{ENTR} &= -\sum_{l=l_{\min}}^{N} p(l) \ln p(l) \\ \text{where } p(l) &= P(l) \Big/ \sum_{l=l_{\min}}^{N} P(l). \end{aligned} \tag{6}$$

The ENTR is considered as a complexity measure of a deterministic structure in a dynamical system. The more complex the deterministic structure, the larger the ENTR value.

A parameter specific to the RP is the cutoff distance ε. If it is too large, almost every point is a neighbor of every other point, which produces a saturation of the RP including irrelevant points; on the contrary, if it is too small, there may be almost no recurrence points, which loses information of the underlying system [22]. Several criteria for choosing the cutoff distance ε have been advocated in the literature [36]. One approach, using a fixed number of neighbors N_n for every point of the trajectory, is called fixed amount of nearest neighbors [22]). In this approach, the cutoff distance ε_i changes for each state x_i to ensure all columns of the RP obtain the same recurrence density. Using this neighborhood criterion, ε_i can be adjusted in such a way that the recurrence rate has a fixed predetermined value (i.e., $\mathrm{RR} = N_n/N$) [22]. In this paper, the DET and ENTR are computed for all 1-s EMG recordings (the number of data $L = 1000$) with a fixed number of neighbors $N_n = 50$. Using this N_n value, the recurrence rate RR is about 0.05.

E. Linear Analysis Methods

In order to compare the extraction information of EMG between linear and nonlinear methods, six well known time-domain and frequency-domain linear methods, i.e., MAV, number of ZC, WL, number of SS changes, mean frequency (MF), and peak frequency (PF) are also used to analyze the sEMG data. For more details, please refer to [14], [37].

F. Adaptive Neuro-Fuzzy Inference System

The adaptive neuro-fuzzy inference system (ANFIS) described by J. Roger [38] is adopted to evaluate the ability and effectiveness of the aforementioned MPE measures in classifying the different seizure phases. The ANFIS learns features in

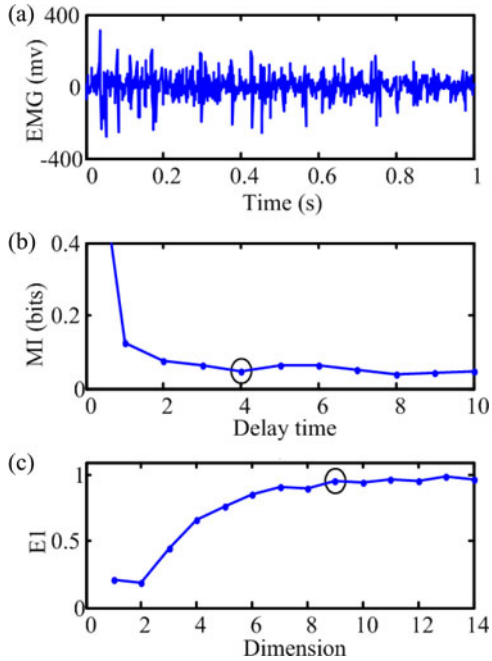

Fig. 2. Phase space reconstruction of a sEMG epochs. (a) an example for sEMG signal; (b) mutual information (MI) versus delay time, the circle in (b) indicates the vicinity of τ, which is at the first local minimum of MI, namely $\tau = 4$; (c) embedding dimension, the circle in (c) indicates $E1$ stops significant changing at the $m = 9$, so take the minimum embedding dimension as 9.

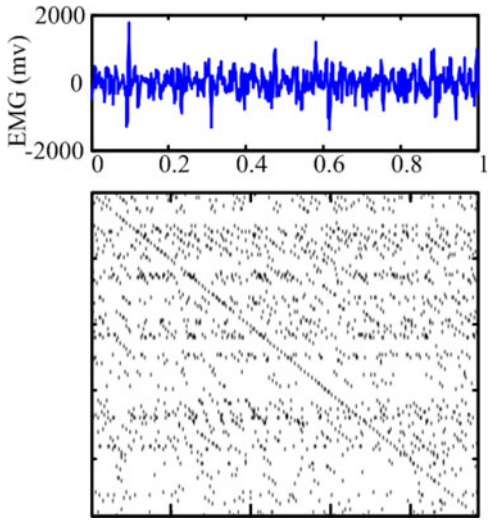

Fig. 3. sEMG epoch from flexor pollicis longus and its RPs from hold and lift a dumbbell (dataset IV).

the data set and adjusts the system parameters according to a given error criterion. It has been widely used in analyzing the biological signals, such as EEG and EMG [39].

In order to improve the generalization, ANFIS classifiers are trained with the back propagation gradient descent method in combination with the least-squares method. For each ANFIS classifier, nonlinear or/and linear features are used as inputs. The samples with target outputs, no action (dataset I), grasp an orange (dataset II), grasp a can (dataset III), and hold a dumbbell (dataset IV) are given the binary target values of (0,0,0,1), (0,0,1,0), (0,1,0,0), and (1,0,0,0), respectively.

III. Results

A. Choice of Time Delay and Embedding Dimension

The first step in the RQA is the reconstruction of the m-dimensional phase space trajectory. The delay time τ and the embedding dimension m of the EMG epochs are determined by using the MI method and the Cao's method. Fig. 2(a) plots an original EMG epoch. Fig. 2(b) shows the mutual information versus the delay time of the EMG, the delay time τ at the first local minimum $\tau = 4$ was selected for the phase space reconstruction. Given the delay time, the Cao method was applied to determine the embedding dimension, the details can be found in [34]. As shown in Fig. 2(c), after the $m = 9$, El is closer to 1 and does not change significantly over the dimension values, as a result we take the minimum embedding dimension as 9 for this EMG epoch.

Next, the MI method and Cao method were applied to all EMG epochs. The optimum values of τ, based on the detection of the first local minimum of the MI function, ranged from 2 to 8 samples (mean and standard deviation is 3.43 ± 1.75) for different EMG epochs. So the optimum delay time $\tau = 4$ was selected for the phase space reconstruction of the four EMG datasets. The optimum embedding dimension m ranged from 6 to 12 (mean and standard deviation are 8.85 ± 1.04) for different EMG segments. Therefore, $m = 9$ is suitable for the topologically proper reconstruction of the EMG data.

B. RQA Measures of sEMG Data

The RPs, as shown in Fig. 3, are constructed from the phase space trajectories of sEMG epochs. Fig. 3 is a representative example of sEMG signals from dataset IV, which recorded at flexor pollicis longus from subject 1. sEMG epoch and its RPs ($m = 9$, $\tau = 4$, and $N_n = 50$) are shown in Fig. 3. Visual inspections of the RPs show that the diagonal lines structure in the RP of sEMG epoch is more regular than ones of dataset I and II sEMG epochs. In order to go beyond the visual impression yielded by RP, the RQA measures DET and ENTR were computed for sEMG epochs. In this example, DET and ENTR value of sEMG is 0.528 and 0.579, respectively.

Further, the RQA measures, DET and ENTR, were applied to analyze all 1280 1 s sEMG epochs in this study (80 $\times$ 4-channel from each dataset I, II, III, and IV). The averages of DET and ENTR of each sEMG epochs are represented as a bar graph, as shown in Fig. 4(a) and (b), respectively. Fig. 4(a) shows the DET values of the grasp of no action are lower than those in the states of grasp and lift an orange, grasp and lift a can, and hold and lift a dumbbell. For example, the DET values for the sEMG epochs from flexor digitorum profundus averaged 0.330 ± 0.105, 0.443 ± 0.094, 0.376 ± 0.077, and 0.563 ± 0.110 (mean $\pm$ SD) in datasets I, II, III, and IV, respectively. The same observation can also be mode for the ENTR

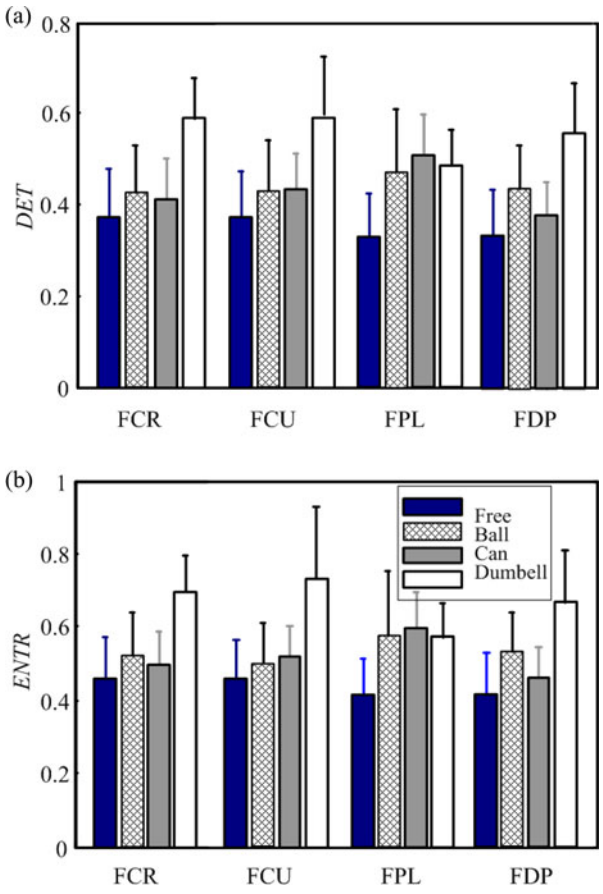

Fig. 4. Bar graph for the DET and ENTR values of the all sEMG epochs, grouped by no action (I), grasp and lift an orange (II) grasp, and lift a can (III) and hold and lift a dumbbell (IV), from flexor carpi radialis (FCR), flexor carpi ulnaris (FCU), flexor pollicis longus (FPL), and flexor digitorum profundus (FDP), respectively. Height of each bar represents mean value, and the horizontal tick above each bar represents standard deviation.

in Fig. 4(b). These observations indicate that the alterations of electrical activity dynamics of muscles could be characterized by the measures of the RQA.

In order to distinguish these observed means statistically, the one-way ANOVA test is performed for the DET and the ENTR values of four different sets. As calculated, the critical value is $F_{\rm crit}(3, 316) = 2.63$ at $\alpha = 0.05$. At this point, the test statistic must exceed to reject the null hypothesis. In order to further investigate the EMG activities of different forearm muscles during hand grasps, statistical analysis of the DET and ENTR values in each dataset were carried out for flexor carpi radialis, flexor carpi ulnaris, flexor pollicis longus, and flexor digitorum profundus, respectively. For example, the results of the DET from flexor digitorum profundus are shown in Table I. It can be seen that the statistical test yields an F-test ($F = 82.0$) that is much higher than the threshold $F_{\rm crit}$ ($F = 2.63$). This suggests the null hypothesis, i.e., no differences of DET between the four different groups from flexor digitorum profundus should be rejected. The similar results of statistical analysis can be obtained from the other tests. The F value is 81.1, 80.5, and 43.8 for the DET from flexor carpi radialis, flexor carpi ulnaris, and flexor pollicis longus, respectively. The F value is 79.2, 82.0, 37.7, and 79.4 for the ENTR from flexor carpi radialis, flexor carpi ulnaris, flexor pollicis longus, and flexor digitorum profundus, respectively. The results suggest that the determinism of sEMG data in the grasps of no action, grasp and lift an orange, grasp and lift a can, and hold and lift a dumbbell are significantly different.

TABLE I
ONE-WAY ANOVA TEST

ANOVA Source of variation	Sums of squares (SS)	Degrees of freedom (DF)	Mean square (MS)	F-test
Between Samples	2.46	3	0.820	82.0 $\boldsymbol{P}$<0.05
Within Samples	3.00	316	0.010	
Total	5.46	319		

TABLE II
ONE-WAY PAIRWISE COMPARISONS VIA SCHEFFE'S TEST

Difference between treatment means	II	III	IV
I	0.113*	0.046*	0.233*
II	-	0.067*	0.120*
III	-	-	0.187*

*Imply that the two treatment level means are statistically different at the $a = 0.05$ level ($S_{\rm th} = 0.036$).

Thus, Scheffe's post-hoc test (MATLAB's multcompare function, statistics toolbox) [40] for all pairwise comparisons between the means is used to determine whether there is statistically significant difference between any two groups. For example, Table II shows the results of multiple comparisons analysis of DET values of sEMG data from flexor digitorum profundus. In this case, the threshold value for Scheffe's post-hoc test can be calculated as follows:

$$S_{\rm th} = \sqrt{\frac{4 \times {\rm MS} \times F_{\rm crit}}{n}} = \sqrt{\frac{4 \times 0.01 \times 2.63}{80}} = 0.036. \tag{7}$$

When the difference between treatment means is larger than the threshold value $S_{\rm th}$, there is a statistically significant difference between these two groups. The DET values for the sEMG epochs from flexor digitorum profundus averaged 0.330, 0.443, 0.376, and 0.563 in datasets I, II, III, and IV, respectively. The results suggest that: the DET values for the sEMG data from flexor digitorum profundus during different types of grasps have significantly higher values than those of no action; grasp an orange and grasp a can have significantly lower values than those of hold a dumbbell; and grasp an orange significantly differs from grasp a can. Similar statistical results can be also obtained from the ENTR values. In short, it can be seen that the difference between different groups is statistically significant.

C. Linear Analysis of sEMG Data

The linear techniques MAV, number of ZC, WL, number of SS changes, MF, and PF, were applied to analyze all 1280 1-s

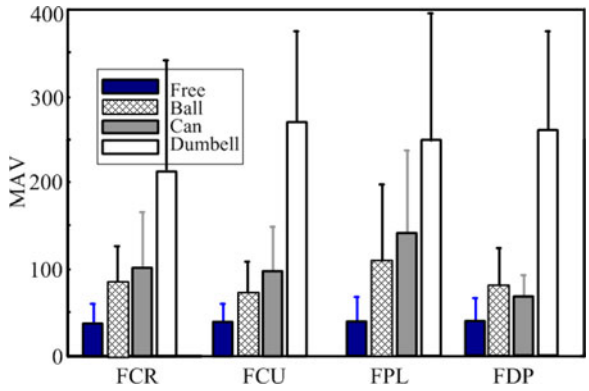

Fig. 5. Bar graph for the MAV of the all sEMG epochs, grouped by no action (I), grasp and lift an orange (II), grasp and lift a can (III), and hold and lift a dumbbell (IV), from flexor carpi radialis (FCR), flexor carpi ulnaris (FCU), flexor pollicis longus (FPL), and flexor digitorum profundus (FDP), respectively. Height of each bar represents mean value, and the horizontal tick above each bar represents standard deviation.

TABLE III
ONE-WAY ANOVA TEST

ANOVA Source of variation	Sums of squares (SS)	Degrees of freedom (DF)	Mean square (MS)	*F*-test
Between Samples	2309607	3	769869	172.4 $P<0.05$
Within Samples	1411307	316	4466	
Total	3720914	319		

TABLE IV
ONE-WAY PAIRWISE COMPARISONS VIA SCHEFFE'S TEST

Difference between treatment means	II	III	IV
I	40.1*	28.2*	216.1*
II		12.1	176.0*
III			187.9*

* imply that the two treatment level means are statistically different at the $a = 0.05$ level ($S_{th} = 24.2$).

sEMG epochs in this study (80 × 4-channel from each datasets I, II, III, and IV). For example, the results of the MAVs are shown in Fig. 5 and the results of one-way ANOVA test for MAV from flexor digitorum profundus are shown in Table III. It can be seen that the statistical test yields an F-test ($F = 172.4$) that is much higher than the threshold F_{crit} ($F = 2.63$). Thereby, this suggests the null hypothesis, i.e., no differences of the MAV between the four different groups from flexor digitorum profundus should be rejected. The similar results of statistical analysis can be obtained from other tests. The F value is 86.0, 203.3, and 85.1 for MAV from flexor carpi radialis, flexor carpi ulnaris, and flexor pollicis longus, respectively. Table IV shows the results of multiple comparisons analysis of MAV values of sEMG data from flexor digitorum profundus. The MAV values for the sEMG epochs from flexor digitorum profundus averaged 39.5, 79.6, 67.7, and 255.6, respectively. It is found that the MAV values for the sEMG data from flexor digitorum profundus during grasping an orange, grasping a can, and holding a dumbbell each are significantly higher than that with no action. The same observation can also be made for the number of ZC, WL, number of SS changes, MF, and PF.

TABLE V
CLASSIFICATION RESULTS WITH LINEAR MEASURES

Desired result	Output result Free	Orange	Can	Dumbbell
Free	78	1	1	0
Orange	0	69	11	0
Can	0	6	74	0
Dumbbell	0	1	1	78

TABLE VI
CLASSIFICATION RESULTS WITH RQA MEASURES

Desired result	Output result Free	Orange	Can	Dumbbell
Free	61	1	18	0
Orange	0	78	2	0
Can	11	6	63	0
Dumbbell	0	0	0	80

D. Classification

The performance of the aforementioned measures to discriminate among groups is also evaluated by means of an adaptive neuro-fuzzy inference system (ANFIS) [38], and tenfold cross-validations are employed to demonstrate the accuracy of classification [41]. First, the ability of the linear techniques in classifying different hand grasp was evaluated using the ANFIS. Four ANFIS classifiers are trained with the back-propagation gradient descent method in combination with the least-squares method when the calculated six linear measures are used as input. Each of the ANFIS classifier is trained so that they are likely to be more accurate for one state of sEMG signals than the other states. Samples with target outputs sets I, II, III, and IV are given the binary target values of (0,0,0,1), (0,0,1,0), (0,1,0,0), and (1,0,0,0), respectively. Each ANFIS classifier was implemented by using the MATLAB software package (MATLAB version 7.0 with fuzzy logic toolbox). The classification results are illustrated in Table V. Out of 320 hand movements in four groups, 299 are classified correctly. The total classification accuracy is 93.4%.

Then, in order to investigate whether or not the RQA measures can effectively extract additional hidden information from sEMG data, the two calculated nonlinear measures are used as the input data in the ANFIS classifiers, and tenfold cross-validations were employed to demonstrate the performance of classification. The classification results are illustrated in Table VI. Out of 320 hand movements in four groups, 282 are classified correctly. The total classification accuracy is 88.1%.

Finally, all the calculated linear and nonlinear measures are used as the input data in the ANFIS classifier. Classification results of the ANFIS model revealed that, as listed in Table VII, only two sEMG segments from the grasp of grasping a can are misclassified by ANFIS as that of grasping an orange sEMG

TABLE VII
CLASSIFICATION RESULTS WITH LINEAR AND RQA MEASURES

Desired result	Output result			
	Free	Orange	Can	Dumbbell
Free	80	0	0	0
Orange	0	79	1	0
Can	0	2	78	0
Dumbbell	0	0	0	80

segments and one sEMG segment from grasping an orange is mistaken as grasping a can. The total classification accuracy of the ANFIS model is 99.1% by using tenfold cross-validations.

IV. DISCUSSIONS

The sEMG signal is a measure of the summed activity of a number of motor unit action potentials (MUAP) lying in the vicinity of the recording electrode, and it may provide insight into the neural activation and dynamics of muscles [42], [43]. The composition of a sEMG signal from MUAPs results in a nonlinear and stochastic signal because of the different firing rates and the large number of motor units that contribute [44]. It is also evident that the sEMG signals are complex data that needs to be condensed with useful information; analysis of sEMG using nonlinear dynamics can provide a better insight into the complex relation between sEMG and muscle activities. In particular, nonlinear sEMG analysis has opened up a range of new perspectives for the study of normal and disturbed neuromuscular functions [29] and their development to a new interdisciplinary field of nonlinear muscle dynamics [45]. Therefore, exploration of hidden dynamical structures within sEMG signals is of both fundamental and clinical interests and has attracted more and more attention [46], [47].

In this study, we have analyzed nonlinear dynamical characteristics in sEMG data during different hand grasp states using the RQA measure. It is found that there is a significant increase of the determinism of the sEMG data from no action grasp state to the selected hand grasp states. Similar results had been reported previously. In [48], the RQA method was applied to indicate the deterministic dynamics of the sEMG signals during the muscle state changes. In [3], the measure DET was used to detect the hidden rhythms in sEMG signals; the high values of the DET in the sEMG signals during the contraction are found, and it was shown that the DET is more effective than median frequency in detecting sEMG changes determined by brisk transients of force output. The increase in determinism is classically attributed to sEMG self-organization into more periodic waves, this process which may be caused by an increase in the probability that motor units will discharge in unity [29].

Furthermore, our results have showed that there is a significant difference in the determinism of the sEMG data from forearm muscles among the states of grasp an orange, grasp a can, and hold a dumbbell. The results in this paper have demonstrated that the DET values for the sEMG data from flexor digitorum profundus have significantly higher values during grasp of hold a dumbbell than during grasp an orange and a can. This finding is consistent with the fact that the contractions of flexor digitorum profundus during hold a dumbbell are stronger than those during grasp an orange and a can. In terms of anatomy, it is well known that the flexor digitorum profundus muscle is a muscle of the human forearm that acts to flex the fingers [49]. Then, the ANFIS is applied to evaluate the performance of nonlinear measures to discriminate among four hand grasp movements. A total classification accuracy of 88.1% is achieved. Moreover, the hand gestures of grasp a can and hold a dumbbell can be separated nicely when using the DET and ENTR measures.

Finally, the classical linear techniques are also used to extract the features from sEMG data. It is found that the high MAVs exist in the sEMG signals during the contraction. These results are consistent with the previous works that muscles in the process of contraction exhibit the increases in sEMG amplitude [14]. Then, the ANFIS is applied to evaluate the performance of linear measures to discriminate among four hand grasp movements. A total classification accuracy of 93.4% is achieved based on the traditional linear techniques. Moreover, it is found that the linear measures can provide a better separability between no action and grasp an object than the nonlinear measures. Additionally, a total classification accuracy of 99.1% is achieved based on the combination of linear and nonlinear measures. Thus, these results suggest that both linear and nonlinear measures of sEMG may contribute to the understanding of the electrical activities of muscle contraction during hand grasp, and our findings provide further support for the notion that different information about muscle electrical activities may be extracted using linear and nonlinear measures. Another significant note is that the RQA measures of a single channel sEMG of 1 s could be calculated in less than 20 ms by using MATLAB (Math Works, Inc.) on a 2.4-GHz personal computer in this study. Therefore the combination of the RQA measures and linear measures in the sEMG data has the potential of providing the basis for designing a real-time hand grasp movement detection system.

It is challenging that employing sEMG, due to its highly dynamic nature, to detect the changes of muscles for musculoskeletal assessment and prosthetic control. It is expected that the reported findings would lead to a solution for sEMG in-depth understanding and further reduction of patients' conscious efforts in monitoring dynamic hand motion of controlled prosthetic devices. One of the future works is targeted to investigate nonlinear classifiers to further improve the classification performance for more natural hand motions [50], [51].

REFERENCES

[1] D. Farina, R. Merletti, and R. M. Enoka, "The extraction of neural strategies from the surface EMG," *J. Appl. Physiol.*, vol. 96, pp. 1486–1495, Apr. 2004.

[2] H. Ghasemzadeh, R. Jafari, and B. Prabhakaran, "A body sensor network with electromyogram and inertial sensors: Multimodal interpretation of muscular activities," *IEEE Trans. Inf. Technol. Biomed.*, vol. 14, no. 2, pp. 198–206, Mar. 2010.

[3] G. Filligoi and F. Felici, "Detection of hidden rhythms in surface EMG signals with a non-linear time-series tool," *Med. Eng. Phys.*, vol. 21, pp. 439–348, Jul./Sep. 1999.

[4] P. K. Artemiadis and K. J. Kyriakopoulos, "An EMG-based robot control scheme robust to time-varying EMG signal features," *IEEE Trans. Inf. Technol. Biomed.*, vol. 14, no. 3, pp. 582–588, May 2010.

[5] Y. H. Yin, Y. J. Fan, and L. D. Xu, "EMG and EPP-integrated human-machine interface between the paralyzed and rehabilitation exoskeleton," *IEEE Trans. Inf. Technol. Biomed.*, vol. 16, no. 4, pp. 542–549, Jul. 2012.

[6] S. Vernon and S. S. Joshi, "Brain-muscle-computer interface: Mobile-phone prototype development and testing," *IEEE Trans. Inf. Technol. Biomed.*, vol. 15, no. 4, pp. 531–538, Jul. 2011.

[7] F. Zhang and H. Huang, "Source selection for real-time user intent recognition towards volitional control of artificial legs," *IEEE J. Biomed. Health Informat.*, 2013, to be published. doi: 10.1109/JBHI.2012.2236563.

[8] C. Cipriani, C. Antfolk, C. Balkenius, B. Rosen, G. Lundborg, M. C. Carrozza *et al.*, "A novel concept for a prosthetic hand with a bidirectional interface: a feasibility study," *IEEE Trans. Biomed. Eng.*, vol. 56, no. 11, pp. 2739–2743, Nov. 2009.

[9] A. Al-Timemy, G. Bugmann, J. Escudero, and N. Outram, "Classification of finger movements for the dexterous hand prosthesis control with surface electromyography," *IEEE J. Biomed. Health Inf.*, vol. 17, no. 3, pp. 608–618, May 2013.

[10] F. V. Tenore, A. Ramos, A. Fahmy, S. Acharya, R. Etienne-Cummings, and N. V. Thakor, "Decoding of individuated finger movements using surface electromyography," *IEEE Trans. Biomed. Eng.*, vol. 56, no. 5, pp. 1427–1434, May 2009.

[11] H. Liu, "Exploring human hand capabilities into embedded multifingered object manipulation," *IEEE Trans. Ind. Inf.*, vol. 7, no. 3, pp. 389–398, Aug. 2011.

[12] S. Kwon and J. Kim, "Real-time upper limb motion estimation from surface electromyography and joint angular velocities using an artificial neural network for human-machine cooperation," *IEEE Trans. Inf. Technol. Biomed.*, vol. 15, no. 3, pp. 522–530, Jul. 2011.

[13] R. Merletti, M. Aventaggiato, A. Botter, A. Holobar, H. Marateb, and T. M. Vieira, "Advances in surface EMG: Recent progress in detection and processing techniques," *Crit. Rev. Biomed. Eng.*, vol. 38, pp. 305–345, 2010.

[14] B. Hudgins, P. Parker, and R. N. Scott, "A new strategy for multifunction myoelectric control," *IEEE Trans. Biomed. Eng.*, vol. 40, no. 1, pp. 82–94, Jan. 1993.

[15] G. Li, A. E. Schultz, and T. A. Kuiken, "Quantifying pattern recognition-based myoelectric control of multifunctional transradial prostheses," *IEEE Trans. Neural Syst. Rehabil. Eng*, vol. 18, no. 2, pp. 185–92, Apr. 2010.

[16] H. B. Xie, J. Y. Guo, and Y. P. Zheng, "Fuzzy approximate entropy analysis of chaotic and natural complex systems: Detecting muscle fatigue using electromyography signals," *Ann. Biomed. Eng.*, vol. 38, pp. 1483–1496, Apr. 2010.

[17] J. Duchene and F. Goubel, "Surface electromyogram during voluntary contraction: Processing tools and relation to physiological events," *Crit. Rev. Biomed. Eng.*, vol. 21, pp. 313–397, 1993.

[18] X. Hu, Z. Z. Wang, and X. M. Ren, "Classification of surface EMG signal with fractal dimension," *J. Zhejiang Univ. Sci. B*, vol. 6, pp. 844–848, Aug. 2005.

[19] J. P. Eckmann and D. Ruelle, "Fundamental limitations for estimating dimensions and lyapunov exponents in dynamic-systems," *Physica D*, vol. 56, pp. 185–187, May 1992.

[20] M. Akay, "Nonlinear biomedical signal processing," in *Dynamic Analysis and Modeling*. vol. II. Piscataway, NJ, USA: IEEE Press, 2001.

[21] X. Zhang, X. Chen, P. E. Barkhaus, and P. Zhou, "Multiscale entropy analysis of different spontaneous motor unit discharge patterns," *IEEE J. Biomed. Health Inf.*, vol. 17, no. 2, pp. 470–476, Mar. 2013.

[22] N. Marwan, M. C. Romano, M. Thiel, and J. Kurths, "Recurrence plots for the analysis of complex systems," *Phys. Rep.-Rev. Sect. Phys. Lett.*, vol. 438, pp. 237–329, Jan. 2007.

[23] G. Ouyang, X. Li, C. Dang, and D. A. Richards, "Using recurrence plot for determinism analysis of EEG recordings in genetic absence epilepsy rats," *Clin. Neurophysiol.*, vol. 119, pp. 1747–1755, Aug. 2008.

[24] M. Bianciardi, P. Sirabella, G. E. Hagberg, A. Giuliani, J. P. Zbilut, and A. Colosimo, "Model-free analysis of brain fMRI data by recurrence quantification," *Neuroimage*, vol. 37, pp. 489–503, Aug. 15, 2007.

[25] H. Yang, "Multiscale recurrence quantification analysis of spatial cardiac vectorcardiogram signals," *IEEE Trans. Biomed. Eng.*, vol. 58, no. 2, pp. 339–347, Feb. 2011.

[26] A. Schmied and M. Descarreaux, "Reliability of EMG determinism to detect changes in motor unit synchrony and coherence during submaximal contraction," *J. Neurosci. Methods*, vol. 196, pp. 238–46, Mar. 30, 2011.

[27] J. L. Dideriksen, D. Falla, M. Baekgaard, M. L. Mogensen, K. L. Steimle, and D. Farina, "Comparison between the degree of motor unit short-term synchronization and recurrence quantification analysis of the surface EMG in two human muscles," *Clin. Neurophysiol.*, vol. 120, pp. 2086–2092, Dec. 2009.

[28] S. M. Rissanen, M. Kankaanpaa, M. P. Tarvainen, A. Y. Meigal, J. Nuutinen, I. M. Tarkka *et al.*, "Analysis of dynamic voluntary muscle contractions in Parkinson's disease," *IEEE Trans. Biomed. Eng.*, vol. 56, no. 9, pp. 2280–2288, Sep. 2009.

[29] C. Morana, S. Ramdani, S. Perrey, and A. Varray, "Recurrence quantification analysis of surface electromyographic signal: Sensitivity to potentiation and neuromuscular fatigue," *J. Neurosci. Methods*, vol. 177, pp. 73–79, Feb. 15, 2009.

[30] C. Yuan, X. Zhu, G. Liu, and M. Lei, "Classification of the surface EMG signal using RQA based representations," in *Proc. IEEE Int. Joint Conf. Neural Netw.*, vol. 1–8, pp. 2106–2111, 2008.

[31] N. H. Packard, J. P. Crutchfield, J. D. Farmer, and R. S. Shaw, "Geometry from a time-series," *Phys. Rev. Lett.*, vol. 45, pp. 712–716, 1980.

[32] H. S. Kim, R. Eykholt, and J. D. Salas, "Nonlinear dynamics, delay times, and embedding windows," *Physica D*, vol. 127, pp. 48–60, Mar. 1999.

[33] A. M. Fraser and H. L. Swinney, "Independent coordinates for strange attractors from mutual information," *Phys. Rev. A*, vol. 33, pp. 1134–1140, Feb. 1986.

[34] L. Y. Cao, "Practical method for determining the minimum embedding dimension of a scalar time series," *Physica D*, vol. 110, pp. 43–50, Dec. 1, 1997.

[35] J. P. Eckmann, S. O. Kamphorst, and D. Ruelle, "Recurrence plots of dynamic-systems," *Europhys. Lett.*, vol. 4, pp. 973–977, Nov. 1987.

[36] L. Matassini, H. Kantz, J. Holyst, and R. Hegger, "Optimizing of recurrence plots for noise reduction," *Phys. Rev. E Stat. Nonlinear Soft Matter Phys.*, vol. 65, Art. no. 021102, Feb. 2002.

[37] G. Fele-Zorz, G. Kavsek, Z. Novak-Antolic, and F. Jager, "A comparison of various linear and non-linear signal processing techniques to separate uterine EMG records of term and pre-term delivery groups," *Med. Biol. Eng. Comput.*, vol. 46, pp. 911–922, 2008.

[38] J. S. R. Jang, "ANFIS—adaptive-network-based fuzzy inference system," *IEEE Trans. Syst. Man Cybern.*, vol. 23, no. 3, pp. 665–685, May/Jun. 1993.

[39] R. T. Lauer, B. T. Smith, and R. R. Betz, "Application of a neuro-fuzzy network for gait event detection using electromyography in the child with cerebral palsy," *IEEE Trans. Biomed. Eng.*, vol. 52, no. 9, pp. 1532–1540, Sep. 2005.

[40] R. V. Hogg and J. Ledolter, *Engineering Statistics*. New York, NY, USA: MacMillan, 1987.

[41] C. D. Katsis, N. Katertsidis, G. Ganiatsas, and D. I. Fotiadis, "Toward emotion recognition in car-racing drivers: A biosignal processing approach," *IEEE Trans. Syst. Man Cybern. A-Syst. Humans*, vol. 38, no. 3, pp. 502–512, May 2008.

[42] X. Li, Y. C. Wang, N. L. Suresh, W. Z. Rymer, and P. Zhou, "Motor unit number reductions in paretic muscles of stroke survivors," *IEEE Trans. Inf. Technol. Biomed.*, vol. 15, no. 4, pp. 505–512, Jul. 2011.

[43] J. S. Karlsson, K. Roeleveld, C. Gronlund, A. Holtermann, and N. Ostlund, "Signal processing of the surface electromyogram to gain insight into neuromuscular physiology," *Philos. Trans. A Math Phys. Eng. Sci.*, vol. 367, pp. 337–356, Jan. 28, 2009.

[44] F. D. Farfan, J. C. Politti, and C. J. Felice, "Evaluation of EMG processing techniques using information theory," *Biomed. Eng. Online*, vol. 9, Art. no. 72, 2010.

[45] H. Geyer and H. Herr, "A muscle-reflex model that encodes principles of legged mechanics produces human walking dynamics and muscle activities," *IEEE Trans. Neural Syst. Rehabil. Eng.*, vol. 18, no. 3, pp. 263–273, Jun. 2010.

[46] P. Palmes, W. T. Ang, F. Widjaja, L. C. Tan, and W. L. Au, "Pattern mining of multichannel sEMG for tremor classification," *IEEE Trans. Biomed. Eng.*, vol. 57, no. 12, pp. 2795–805, Dec. 2010.

[47] D. Rodrick and W. Karwowski, "Nonlinear dynamical behavior of surface electromyographical signals of biceps muscle under two simulated static work postures," *Nonlinear Dyn. Psychol. Life Sci.*, vol. 10, pp. 21–35, Jan. 2006.

[48] C. L. Webber, Jr., M. A. Schmidt, and J. M. Walsh, "Influence of isometric loading on biceps EMG dynamics as assessed by linear and nonlinear tools," *J. Appl. Physiol.*, vol. 78, pp. 814–822, Mar. 1995.

[49] G. R. Naik, D. K. Kumar, and Jayadeva, "Twin SVM for gesture classification using the surface electromyogram," *IEEE Trans. Inf. Technol. Biomed.*, vol. 14, no. 2, pp. 301–308, Mar. 2010.

[50] Z. Ju and H. Liu, "Fuzzy Gaussian mixture models," *Pattern Recognit.*, vol. 45, pp. 1146–1158, 2012.

[51] Z. Ju and H. Liu, "Human hand motion analysis with multisensory information," *IEEE/ASME Trans. Mechatron.*, 2013, to be published. doi:10.1109/TMECH.2013.2240312.

Gaoxiang Ouyang received the B.S. degree in automation and the M.S. degree in control theory and control engineering both from Yanshan University, Hebei, China, in 2002 and 2004, respectively, and the Ph.D. degree from the Department of Manufacturing Engineering, City University of Hong Kong, Hong Kong, in 2010.

He is currently a Lerverhulme Visting Fellow in the intelligent systems and biomedical robotics group at the University of Portsmouth, Portsmouth, U.K. His research interests include bio-signal analysis, neural engineering, and dynamics system. He has published numerous refereed international journals and conference papers.

Xiangyang Zhu received the B.S. degree from the Department of Automatic Control Engineering, Nanjing Institute of Technology, Nanjing, China, in 1985, the M.Phil. degree in instrumentation engineering, and the Ph.D. degree in automatic control engineering, both from Southeast University, Nanjing, China, in 1989 and 1992, respectively.

From 1993 to 1994, he was a Postdoctoral Research Fellow with Huazhong University of Science and Technology, Wuhan, China. He joined the Department of Mechanical Engineering as an Associate Professor, Southeast University, in 1995. Since June 2002, he has been with the School of Mechanical Engineering, Shanghai Jiao Tong University, Shanghai, China, where he is currently a Changjiang Chair Professor and the Director of the Robotics Institute. His current research interests include biomechatronics, human-machine interfacing, and robotic manipulation planning. He received the National Science Fund for Distinguished Young Scholars in 2005.

Zhaojie Ju (M'08) received the B.S. degree in automatic control and the M.S. degree in intelligent robotics both from the Huazhong University of Science and Technology, Hubei, China, in 2005 and 2007, respectively, and the Ph.D. degree in intelligent robotics at the University of Portsmouth, Portsmouth, U.K., in 2010.

He is currently a Lecturer in the School of Creative Technologies, University of Portsmouth. He previously held research appointments in the Department of Computer Science, University College London and Intelligent Systems and Biomedical Robotics group, University of Portsmouth, U.K. His research interests include machine intelligence, robot learning, pattern recognition and their applications in robotic/prosthetic hand control, and human-robot interaction.

Honghai Liu (M'02–SM'06) received the Ph.D. degree in robotics from King's College London, London, U.K., in 2003.

He is currently a Professor of intelligent systems at the University of Portsmouth, Portsmouth, U.K. He previously held research appointments at the Universities of London and Aberdeen, and Project Leader appointments in large-scale industrial control and system integration industry. His research interests include biomechatronics, pattern recognition, intelligent video analytics, intelligent robotics, and their practical applications with an emphasis on approaches that could make contribution to the intelligent connection of perception to action using contextual information.